Original Research Article

REFRACTIVITY GRADIENT VARIATIONS AND INTERTROPICAL DISCONTINUITIES ACROSS NIGERIA.

Abstract

The complexity of the troposphere has a significant impact on radio signal transmission. This has led to the computation of refractivity gradients, which is an important parameter for the estimation of path clearance and propagation effects such as super-refraction, sub-refraction and ducting. This research focuses on the interrelationships that exist between Refractivity Gradient and Intertropical Discontinuity (ITD). The ITD is a major phenomenon that determines the weather in West Africa. The refractivity gradient was calculated using hourly data of temperature and relative humidity for the years 2017 and 2018 taken at two levels (surface and 1000hpa) collected from the archives of the European Centre for Medium-Range Forecasts (ECMWF) for twenty meteorological stations in Nigeria. The refractivity gradient values obtained were used to characterize the atmospheric conditions of the stations diurnally and seasonally. Results showed that during the dry season, the atmosphere is sub-refractive at the coastal and derived savannah regions while during the rainy season, super-refractive conditions prevails. At the guinea and sub-Sahelian regions the atmosphere is mostly sub-refractive. Diurnal variations show that the coastal and derived savannah regions have atmosphere that are super refractive throughout the day, the guinea savannah regions are characterized by the atmosphere that is super-refractive in the early morning hours and sub-refractive between late morning and afternoon periods. These occurrences are found to be greatly influenced by the north-south trajectory of the Intertropical Discontinuity. Using the ANOVA method, five regression models (Linear, Cubic, Quadratic, Power and Log) were developed between refractivity gradient and ITD. The linear model ($L = B_0 + B_1RG$) are mostly significant with coefficient of determination ranging between 97% and 99%) across all the regions.

Keywords: Refractivity Gradient, Intertropical Discontinuity.

1. Introduction

The relationship between surface refractivity, refractivity gradient, and radio refractivity is complex and interconnected. Surface refractivity refers to the refractive index observed at the Earth's surface, which is influenced by various atmospheric conditions such as temperature, pressure, and humidity (Emetere et al. 2021). On the other hand, the refractivity gradient measures the vertical change in refractivity concerning height in the atmosphere (Akpootu & Rabiu, 2019). Fluctuations in atmospheric conditions can affect the refraction of radio waves, which in turn influences radio refractivity (Dairo et al. 2020).

The combination of surface refractivity and refractivity gradient collectively determines total radio refractivity, which plays a crucial role in the propagation characteristics of radio waves in the atmosphere. Changes in surface refractivity and refractivity gradient can induce fluctuations in radio refractivity, leading to variations in signal propagation, fading, and interference in wireless communication systems (Benzon & Høeg, 2015).

Numerous scientific studies have investigated the correlation between surface refractivity, refractivity gradient, and radio refractivity in different scenarios. Akpootu and Rabiu (2019) developed empirical models to estimate tropospheric radio refractivity in Osogbo, Nigeria, considering atmospheric variables such as pressure, humidity, and temperature. Dairo et al. (2020) examined the impact of tropospheric scintillation on satellite links across different climatic zones in Nigeria, where the refractivity gradient plays a role.

Abnormal propagation conditions, such as multipath fading and significant signal enhancement on line-of-sight links, or interference on trans-horizon paths, can be better identified using the spatial distribution of vertical refractivity gradient and ducting index (Emmanuel et al. 2020). These abnormal conditions can result in decreased signal strength, reduced reliability, and degraded quality of wireless communication.

When designing radio systems, the radio refractivity gradient is a crucial parameter to consider. Strong negative gradients, known as super-refraction, can cause interference between terrestrial stations, while positive gradients, known as sub-refraction, can affect the lowest detectable signal level. Understanding the distribution and variability of the surface refractivity gradient is essential for optimal performance in radio systems (Salamon et al. 2014; Bettouche et al. 2020).

The Intertropical Discontinuity (ITD) serves as a transition zone between humid maritime air masses and dry continental air masses (Ayanlade et al. 2019). It is characterized by a significant gradient in atmospheric variables such as temperature, humidity, and refractivity (Ayanlade et al. 2019; Pospichal et al. 2009). The movement of the ITD affects the unpredictability and intensity of the "Little Dry Season" in southern Nigeria, as it is related to variations in rainfall patterns (Adejuwon & Odekunle, 2006). The ITD acts as a barrier between the humid maritime air mass and the continental air mass of the Harmattan (Schneider et al. 2014).

The intertropical discontinuity contributes to the formation of the refractivity gradient due to temperature and humidity variations. Research conducted by Dairo et al. (2017) used radiosonde

data to investigate the refractivity gradient across the ITD. The refractivity gradient is more pronounced in areas influenced by the intertropical discontinuity zone due to significant temperature and moisture content differences among trade wind systems (Lawal et al. 2023).

The intertropical discontinuity also affects radar systems operating in tropical regions through its influence on the refractivity gradient. López et al. (2018) researched the impact of the ITD on the performance of weather radar. They found that fluctuations in the refractivity gradient over the ITD can introduce errors in radar data, affecting the accuracy of rainfall estimation and storm tracking**.**

2. Methodology

Temperature and relative humidity readings were collected hourly at the surface and at a height of 1 km with an equivalent pressure of 1000 hpa during two (2) years of Era Interim data collection (2017-2018). These data, which had a resolution of 0.25x0.25, were obtained from the archives of the European Centre for Medium-Range Forecasts (ECMWF). They were used for this research, and they were dispersed over twenty stations that were located in each of Nigeria's four climatic areas: the Coastal, Derived, Guinea, and Sub-Sahel regions.

When calculating the ITD (Intertropical Discontinuity) mean monthly locations across Nigeria, the dewpoint temperature readings were collected at the same height and with the same resolution for all of the readings.

Refractivity and Refractivity Gradient

To estimate the radio refractivity gradient, of the lowest 1 km of the troposphere, each ascent data was grouped such that between the surface and 1 km was classified as the lowest 1 km. The value of radio refractivity was computed from equation 3.1. The refractivity gradient data of the lowest atmospheric layers within the range of 0-1 km, ΔN_{1km}, were computed using equation (3.2). The value of the radio refractivity gradient obtained was used to characterize the refractive propagation conditions of the lowest atmosphere into sub-refraction$\left(\frac{\Delta N}{\Delta h} > -40\right)$, super-refraction $\left(\frac{\Delta N}{\Delta h} < -40\right)$, and ducting $\left(\frac{\Delta N}{\Delta h} < -157\right)$. The refractivity gradient value is thus presented in the results and discussion.

The variation of refractivity gradients (dN) is a function of climate, season, and transient weather conditions across the day and terrain over the communication path (Dominguez *et. al,* 1998). The negative value of refractivity gradients (beyond 100 N-unit/km) causes the radio signal to bend toward the earth and to traverse beyond the geometric horizon (super-refraction). When it becomes positive, it is known as sub-refraction and can cause diffraction loss (Emmanuel et al., 2018).

The Refractivity (N) which is the physical property of a medium as determined by its index of refraction is denoted by;

$$N = (n-1) \times 10^6$$

The refractive index of air, denoted as n, exhibits a deviation from unity that is limited to a small fraction of a few parts per ten thousand (Freeman et al.; 2007).

The radio refractivity, denoted as (N) as recommended by ITU, is determined by the combined dry and wet parametric values, and may be mathematically represented as;

$$N = 77.6\frac{P}{T} + 3.73X10^5\frac{e}{T^2} \text{ (N-units)} \quad (3.1)$$

Equation (1) above is divided into two parts

$$N = N_{DRY} + N_{WET} \quad (3.2)$$

where,

$$N_{DRY} = 77.6\frac{P}{T}$$

$$N_{WET} = 3.73X10^5\frac{e}{T^2}$$

where,

- P= atmospheric pressure (hpa),
- e = water vapour pressure (hpa),
- T= absolute temperature (K)

The differential equation that describes the relationship between the water vapour pressure, e (hPa), the saturation vapour pressure, es (hPa), and the relative humidity, H (%), may be derived from equation (3.1) as follows:

$$e = \frac{H}{100}es \quad (3.3)$$

where,

$$es = a \exp\left[\frac{bt}{t+c}\right] \quad (3.4)$$

The values of the coefficients in equation (3.4) are obtained as a = 6.1121, b = 17.502, c = 240.97. The atmospheric temperature, denoted as T, is measured in Kelvin (K), whereas the dry atmospheric pressure, is represented by P in (hPa). Additionally, the temperature, is denoted as t in (°C).

Hence, the Refractivity Gradient in N-units per km may be represented as :

$$G = \frac{dN}{dh} = \frac{N_{1km} - N_s}{\Delta h} \quad (3.5)$$

Where N_{1km} *is* the refractivity at 1 km height is, N_s is the refractivity at the surface, Δh is the change in height.

The connection between the Latitudinal (L) location of the Intertropical discontinuity (ITD), which is the independent variable, and the Refractivity Gradient (RG), which is the dependent variable, was investigated using five regression models in this work.

REGRESSION LINE. EQUATIONS ADOPTED

a. LINEAR: $L = B_0 + B_1 R_G$ (3.6)
where B_0 is the intercept and B_1 is the slope

b. QUADRACTIC: $L = RG^2 + RG + B_0$ (3.7)

c. CUBIC: $L = -RG^3 - RG^2 - RG - B_0$ (3.8)

d. LOG: $LnRG = - B_0 + B_1 LnL$ (3.9)

e. POWER: $RG = - B_0 + B_1 LnL$ (4.0)

3. Results and Discussion

SPATIAL DISTRIBUTION OF REFRACTIVITY GRADIENT ACROSS NIGERIA LATE DRY SEASON PERIOD

The seasonal variations of the radio refractivity gradient are presented in Figure 1 which shows the Late dry season months of (December - February) which are dominated by very little rainfall, the results obtained indicated variations at the different stations, having their maximum values at the Sahel regions indicating sub-refractions with positive values ranging from (25.704 – 105.8) The values are lesser in the coastal regions which are dominated by super-refractions, the guinea savanna regions such as minna, bida, jos are partly sub-refractive and super refractive while the derived regions such as Ilorin, Abeokuta are significantly dominated by super refractions for the period of December-February.

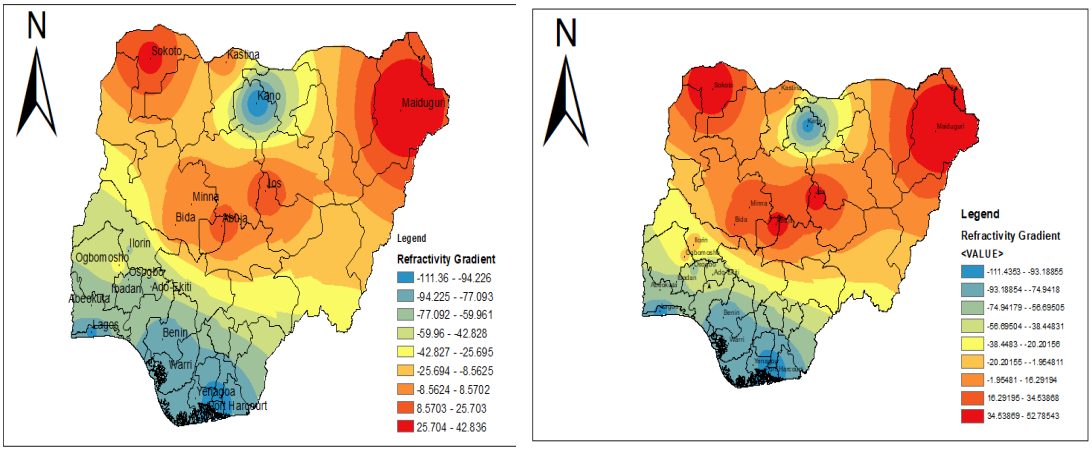

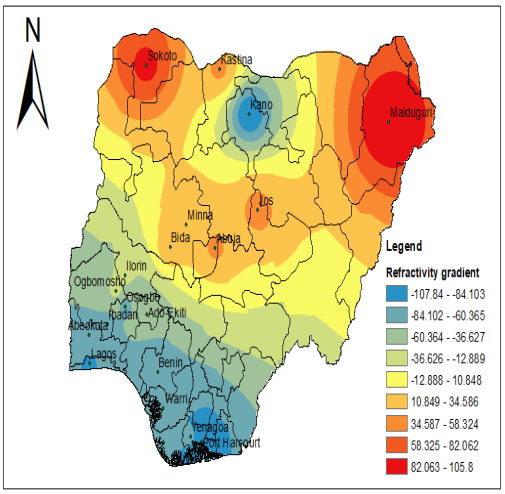

FIG 1: Spatial distribution of Refractivity Gradient across Nigeria in the late dry season of December, January and February

EARLY RAINY SEASON

The seasonal variation of the radio refractivity gradient is presented in Figure 2, as we move inland the values of the refractivity gradient increase. The Coastal and derived savannah regions were super-refractive due to the high level of humidity in the atmosphere as a result of rainfall, while the Guinea and Sahel savannah regions were sub-refractive as a result of the low amount of humidity attributed to very low rainfall in these regions at the early raining season months.

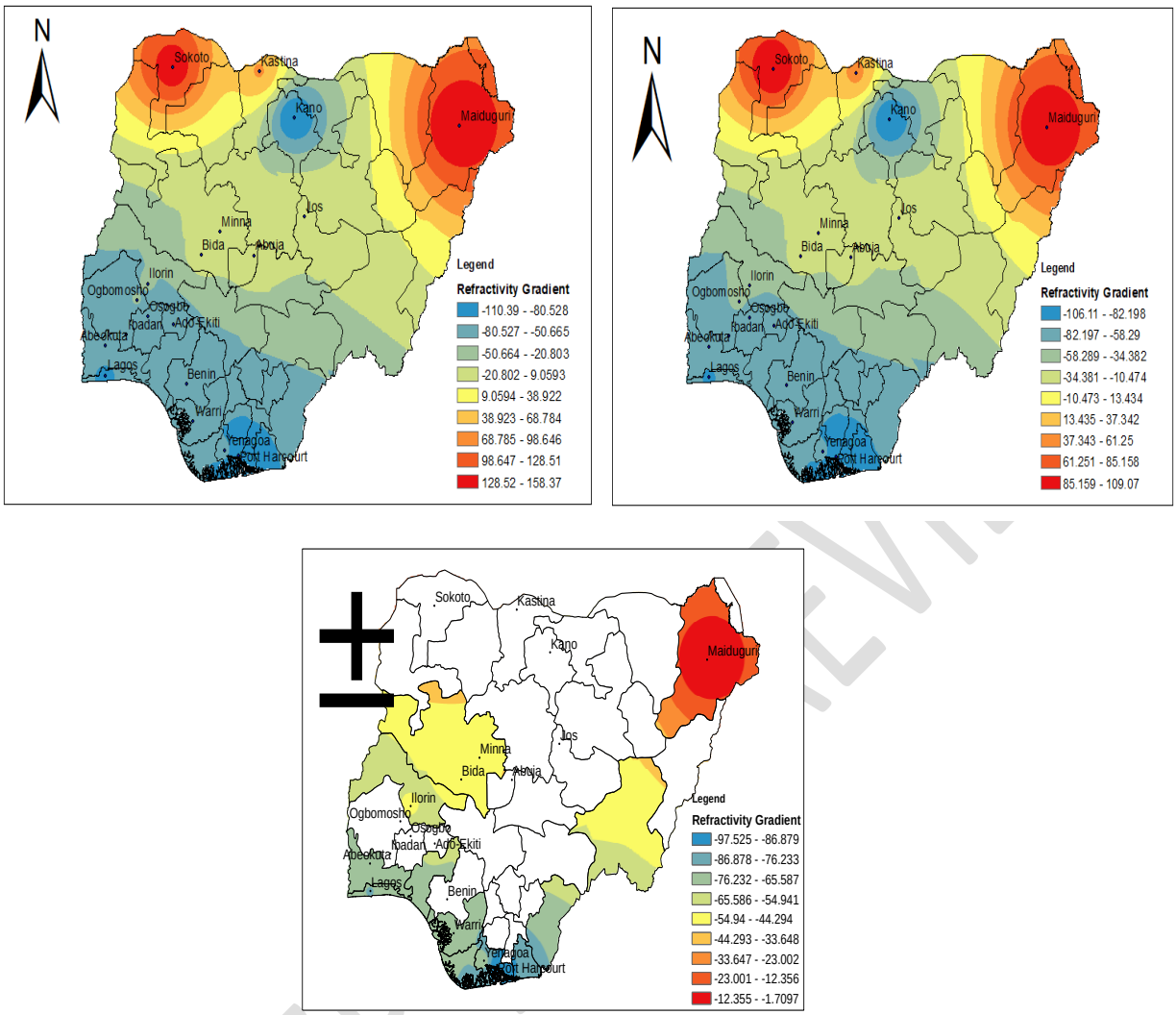

FIG 2: Spatial distribution of Refractivity Gradient across Nigeria in the early rainy season of March, April and May

LATE RAINY SEASON

The atmosphere across Nigeria during this period is Super-refractive as shown in Fig 3 below due to the rainfalls that dominated the nation around this period. The values of the refractivity gradient increase as we move from south to north across the Nation.

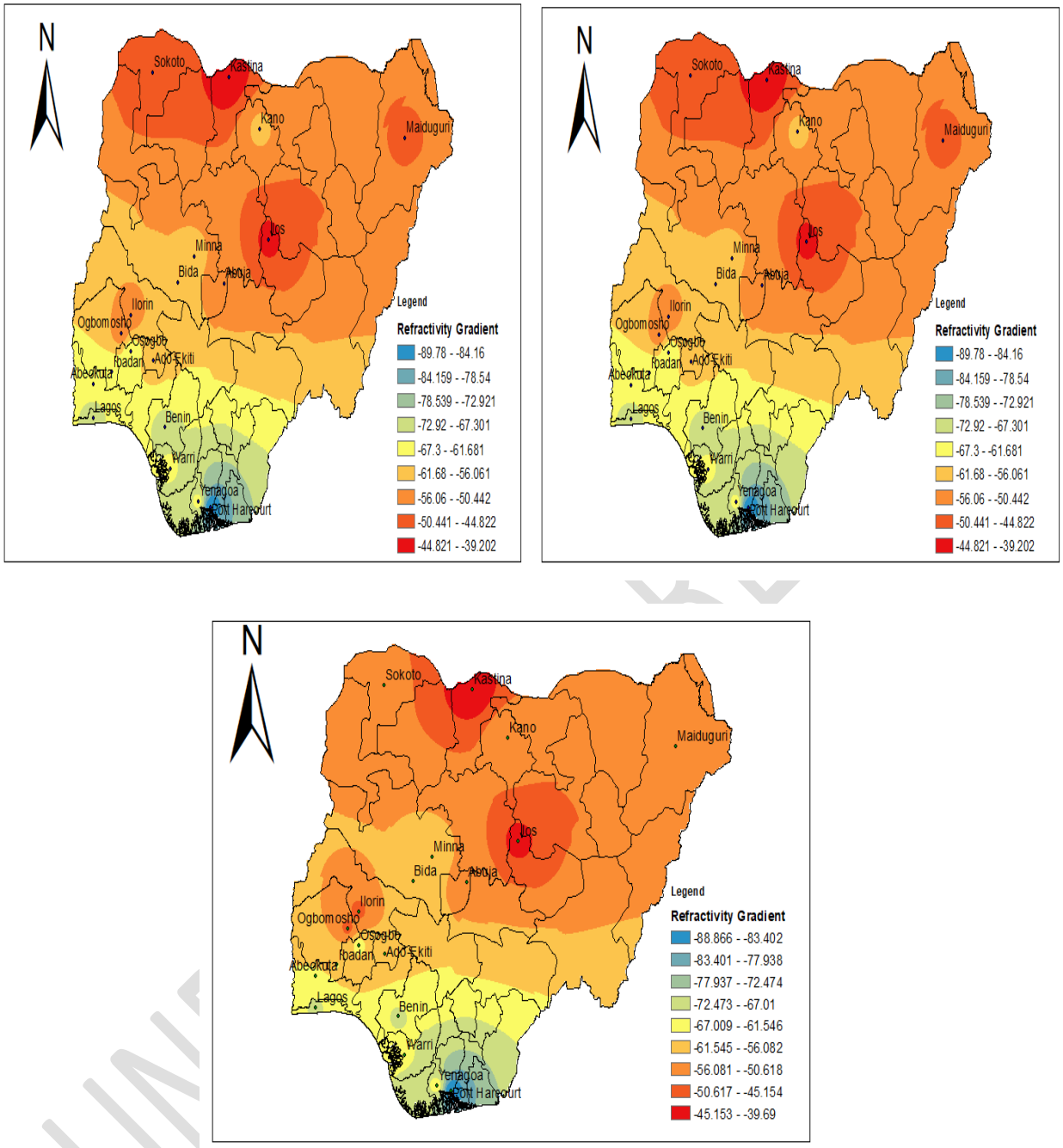

FIG 3: Spatial distribution of Refractivity Gradient across Nigeria in the late Rainy season of June, July and August

EARLY DRY SEASON

The atmosphere in the coastal and derived regions was Super-refractive in this period which can be attributed to the humid atmosphere and the influence of the water bodies present around these regions. The reverse is the case in the Guinea

savanna and Sub-Sahelian regions which were Sub-refractive as shown in Fig 4 below with the exception of Kano which was super-refractive, the presence of water bodies such as Jakara River and Kusalla dam in this area seems to be the major reason why the atmosphere here was super-refractive.

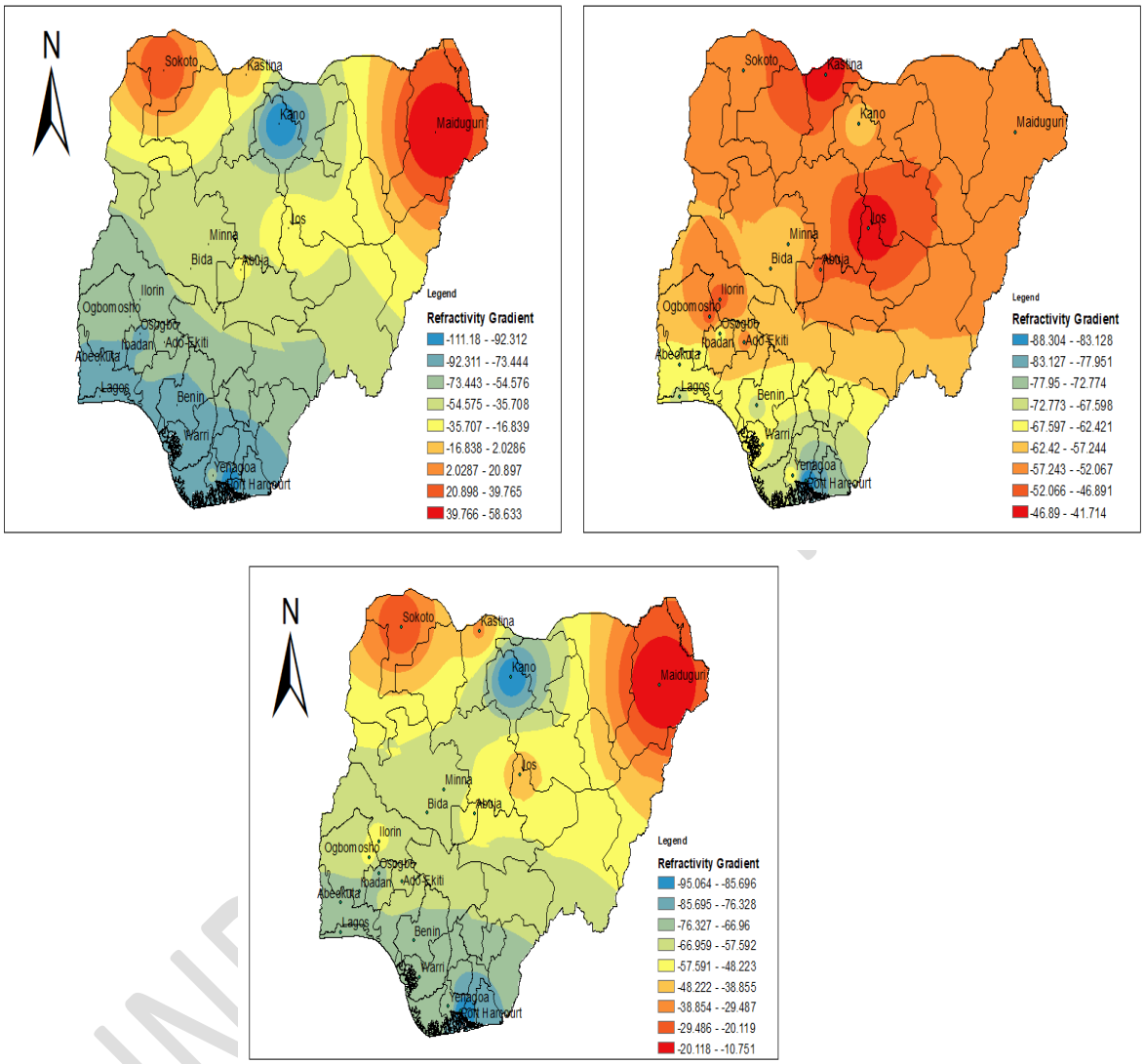

FIG 4: Spatial distribution of Refractivity Gradient across Nigeria in the Early dry season of September, October and November

INTERCONNECTION BETWEEN REFRACTIVITY GRADIENT AND INTERTROPICAL DISCONTINUITY

The climate of the Earth is not dependent on the fact that sunlight is evenly distributed around the equator. Climatic irregularities are significant in the eastern tropical Pacific and Atlantic Oceans where the regions of maximum sea surface temperature, convective cloud cover, and rainfall occur north of the equator. This is the result of two sets of factors: interactions between the ocean and atmosphere that are capable of convening balance into imbalance, and the geometries of the continents that determine in which longitudes the interactions are effective and in which hemisphere the warmest waters and the intertropical discontinuity is located. Where the transition zone is shallow, winds can easily impact the sea surface temperature, making for optimal ocean-atmosphere interactions. The convective shoreline in the tropical Atlantic and Pacific to the east, but not in the Indian Ocean, since the former is dominated by easterly trade winds and the latter by monsoons, which have a much bigger meridional component.

JANUARY-FEBRUARY

In January-March as seen in Fig 5, the seasonal variation of the radio refractivity gradient is presented along with the Intertropical discontinuity (ITD) for January. The position of ITD, covers the coastal and a large part of the derived regions as shown in Fig 5 below, even though January to February is known to be a dry month, it can be deduced that little amount of rainfall can still be experienced in the coastal and derived regions. The atmosphere in the coastal and derived regions in this month was super-refractive while regions above ITD were sub-refractive.

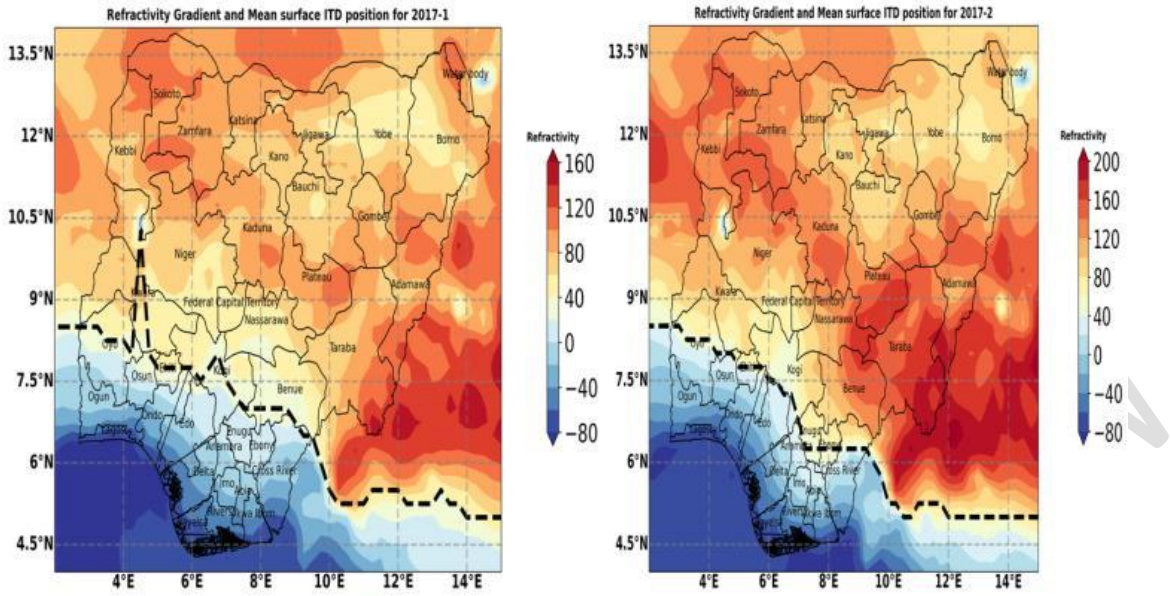

fig 5. Refractivity Gradient and mean surface ITD position for 2017-1 and 2017-2

Observations:

- The month is dry and less humid at the north as shown through the position of ITD here.
- Only coastal and derived regions may experience very little amount of rainfall

MARCH – APRIL

In April, the position of ITD as shown below, shifted further north covering the coastal, derived Guinea savannah. This month was majorly characterized by heavy rainfalls all over the regions covered by the ITD position as shown below in Fig 6; the coastal, derived and Guinea savannah regions remain super-refractive. The sub-sahelian region was sub-refractive

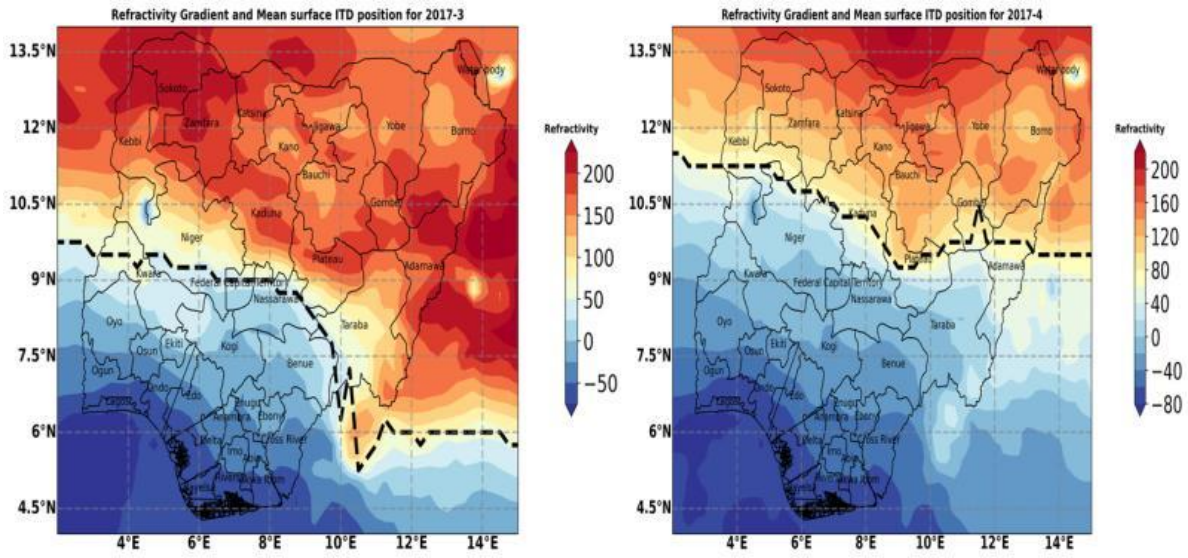

Fig 6. Refractivity Gradient and mean surface ITD position for 2017-3 and 2017-4

Observations:

- The position of ITD divides the nation into sub-refraction and super-refraction, with the stations above the line experiencing sub-refraction and areas below it experiencing super-refraction.
- Rainfalls were observed at stations below the line reducing the values of refractivity gradient.

MAY - JUNE

ITD position shifted above Nigeria, cutting through a fraction of the Sub-sahelian region over the land through Yobe and Borno in May and disappeared completely in June as shown below in Fig 7-9; this implies that all stations across Nigeria will experience rainfall. All regions were super-refractive

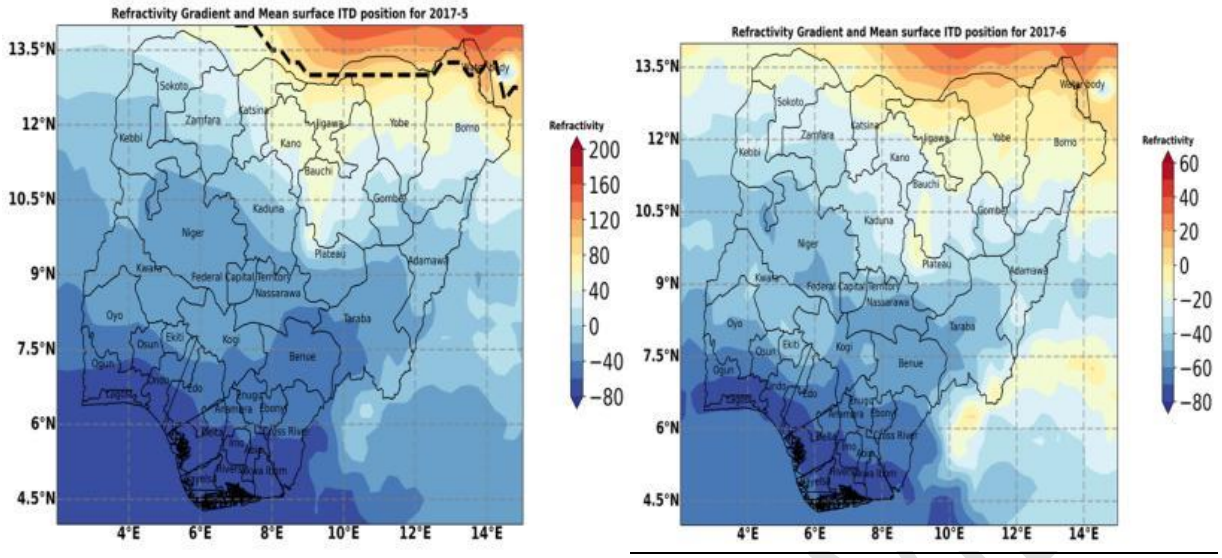

Fig 7. Refractivity Gradient and mean surface ITD position for 2017-5 and 2017-6

Observations:

- The ITD position was rarely seen across Nigeria.
- Parts of the sub-sahelian region may exhibit both super and sub-refractions.
- Due to the low values of refractivity across the stations, there is even a distribution of heavy rainfall across all stations.

JULY-SEPTEMBER

From July to September, the position of ITD remains above Nigeria, which indicates the presence of rainfall all over Nigeria as shown below in Fig 8, the values of refractivity in this period increase over the northern part of the nation. The atmosphere remains super-refractive around this period due to the continuation of rainfall experienced from May to June.

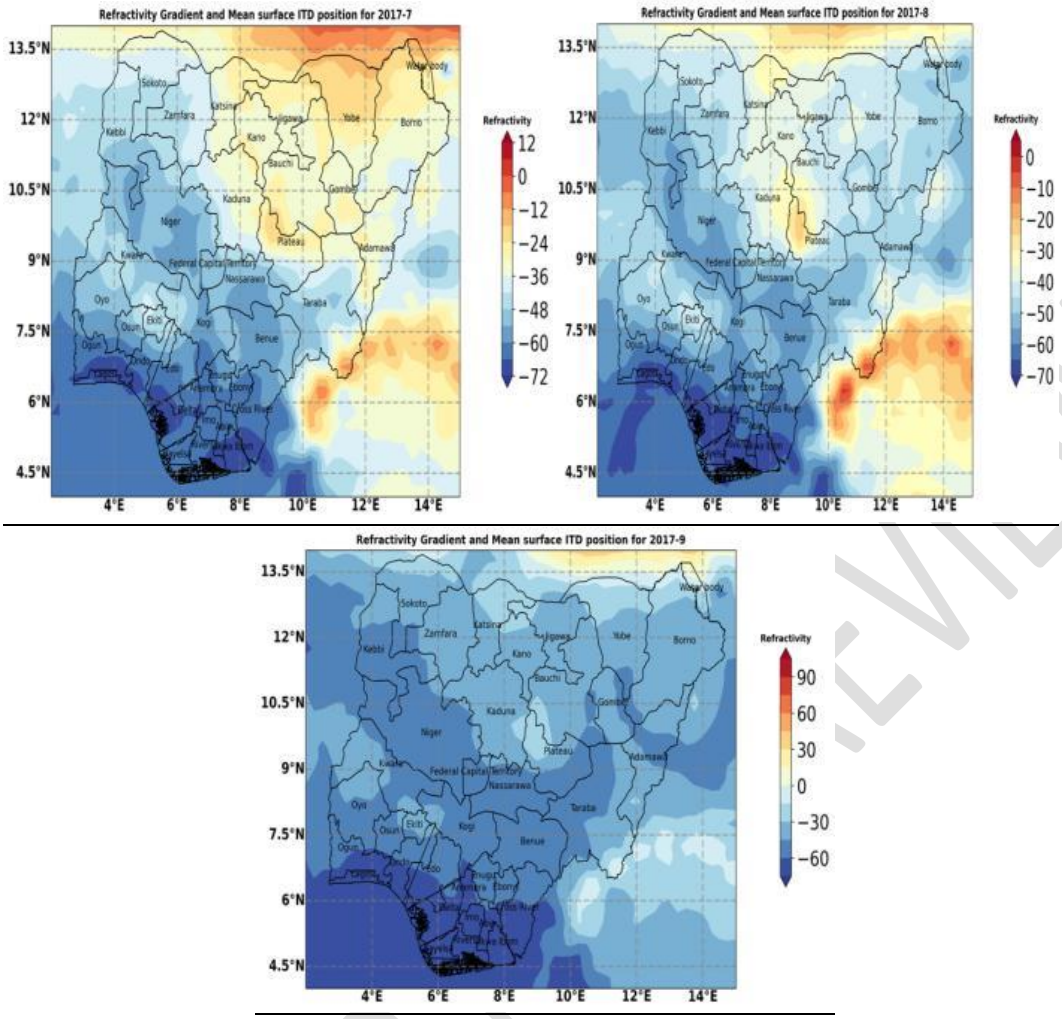

Fig 8. Refractivity Gradient and mean surface ITD position for 2017-7, 2017-8 and 2017-9

OCTOBER-DECEMBER

In November, the ITD position shifted further south of Nigeria, regions below the line remained super-refractive while those above were sub-refractive.

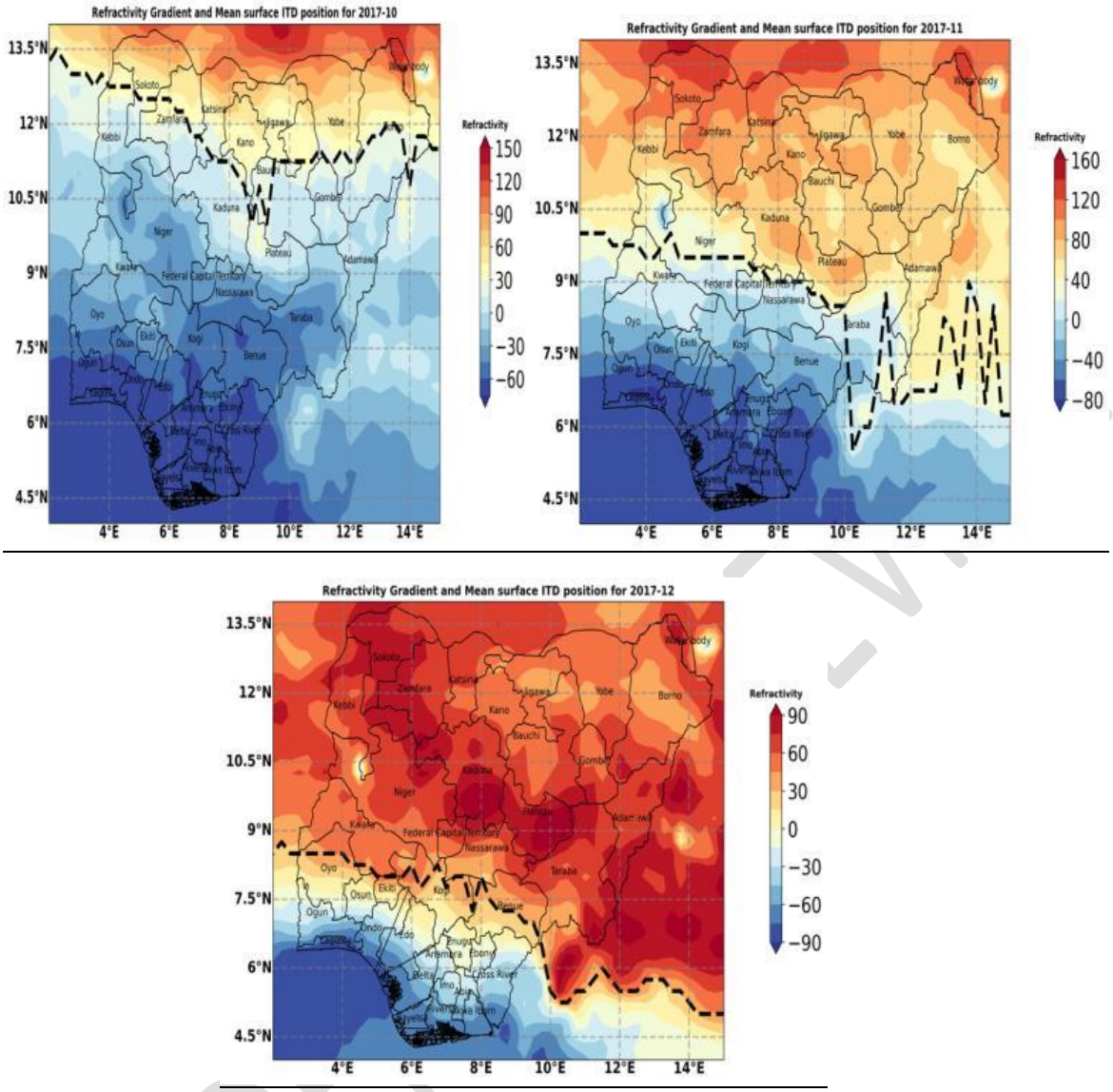

Fig 9. Refractivity Gradient and mean surface ITD position for 2017-10, 2017-11 and 2017-12.

Observations:

- These seasons introduces the dry hammattan wind from the north to every parts of the country.
- As deducted from ITD position in this month, the continental air masses winds dominates the nation which depicts the dryness experienced in these months.
- Coastal regions atmosphere will be dry and moist due to the humid atmosphere as a result of the presence of water bodies such as rivers, lakes and the Atlantic

ocean with the effects of the dry wind.

4. MODELS OF REFRACTIVITY GRADIENT AND INTERTROPICAL DISCONTINUITY ACROSS NIGERIA

To test the research question, a linear and multiple regression was conducted, with ITD parameters such as; mean daily values of Latitudes, longitudes and dewpoint temperatures modelled against mean daily values of Refractivity Gradient, it was discovered that only the latitudinal positions of the Intertropical Discontinuity were suitable for these models while other parameters like dewpoint temperatures, longitudinal positions were insignificant for both linear and multiple regressions adopted in this work as calculated in the tables shown below across the various regions in Nigeria;

L (latitudinal position of ITD) is the independent variable or predictor in these models while Refractivity Gradient is the dependent variable. The model performed better in the Derived and Guinea savannah regions with about 98% coefficient of determination followed by Sahel, Coastal regions with a 97% coefficient of determination. All of the predictors explain a large amount of the variance between the variables. R^2 = 0.984-0.973) across all stations; it shows that the variability of L is explained by 97-98% of the variance of RG, the coefficient of multiple correlation (R) = 0.986 explains the strong correlation between the predicted data and the observed data.

COASTAL	N	B_0	SEB_0	B_1	SEB_1	R	R^2	F	P-value
LINEAR	365	34.796	6.89	0.252	554e-6	0.972	0.973	12882	0.0000
QUADRATIC	365	49.310	43.097	0.591	0.012	0.992	0.984	11608	1.7e181
CUBIC	365	-20.925	-76.925	-0.245	-0.027	0.996	0.992	15857	3.24e-8
POWER	365	-206.193	-170.315	47.611	15.664	0.991	0.983	20856	0.0000
LOG	365	-5.824	-0.069	0.549	2.6e-4	0.986	0.972	12837	0.0000

Table 1. shows the regression model analysis for coastal regions

DERIVED	N	B_0	SEB_0	B_1	SEB_1	R	R^2	F	P-value
LINEAR	365	46.430	11.286	0.6027	259e-5	0.992	0.982	19,582	0.0000
QUADRATIC	365	64.760	130.038	1.269	0.093	0.994	0.985	12,080	3.13e-18
CUBIC	365	-175.029	-2457	-11.833	-9.040	0.997	0.992	14,699	7.13e-33
POWER	365	-105.739	-37.537	19.995	2.839	0.994	0.982	19,935	0.0000
LOG	365	-4.9135	-0.039	0.3599	115e-5	0.915	0.972	12,686	0.0000

Table 2. shows the regression model analysis for the Derived regions

GUINEA	N	B_0	SEB_0	B_1	SEB_1	R	R^2	F	P-value
LINEAR	365	15.130	0.4796	0.1099	813E-7	0.992	0.984	22,009	0.0000
QUADRATIC	365	14.909	0.443	0.1218	125e-6	0.994	0.989	17,188	1.09e-30
CUBIC	365	15,177	0.4356	0.1289	116e-6	0.997	0.994	19,190	5.1e-8
POWER	365	-296.249	-463.630	110.129	68.776	0.994	0.989	31,101	0.0000
LOG	365	-22.558	-11.103	8.497	1.665	0.915	0.838	1,872	0.000

Table 3. shows the regression model analysis for Guinea regions

SAHEL	N	B_0	SEB_0	B_1	SEB_1	R	R^2	F	P-value
LINEAR	365	11.944	0.334	0.0491	1.62e-5	0.991	0.983	20,865	0.0000
QUADRATIC	365	11.642	0.403	0.048	1.49e-5	0.994	0.988	14,619	0
CUBIC	365	11.490	0.299	0.055	27e-6	0.998	0.994	18,695	2.96e-65
POWER	365	596.790	2381.79	245.932	391.523	0.993	0.985	23,853	0.0000
LOG	365	-29.397	-11.406	12.003	1.858	0.971	0.943	6,013	0.000

Table 4. shows the regression model analysis for the Sahel regions

VALIDATIONS OF MODEL (ACTUAL VS PREDICTED VALUES OF REFRACTIVITY GRADIENTS)

In other to test the values and significancy of the models generated in the tables above, the mean daily value of Intertropical discontinuity for the year 2020 was computed and the various values were completely used to generate the values of Refractivity Gradients and the results were compared to the actual values of Refractivity gradients across the stations for that year. Using the linear relationship generated across the coastal regions in the table above.

L = 34.796 + 0.252RG, for example, the following values were computed across the coastal region for;

Jan 1 2020 : L was 6.771°N, actual RG -115.1460 we can now calculate the predicted RG using ;

$$L = 34.796 + 0.252RG$$

$$RG = \frac{L - 34.796}{0.252RG} = -111.210$$

The difference between the actual and precited as calculated above in the coastal region is -3.936 but reduces as we transit from the rainy season to the dry season. The validation was stronger in the late dry season.

COASTAL REGION

The correlation coefficient in this region is 0.9862, the correlation is positive. It shows there is a strong linear relationship between Actual RG and Predicted RG. As Actual RG increases, Predicted RG also appears to increase. While R^2 suggests that 97% of changes in Actual RG to changes in Predicted RG, 3% are unexplained which justifies that this model can be used to forecast future values of Refractivity gradients provided that the latitudinal position of ITD is known for stations in the coastal region.

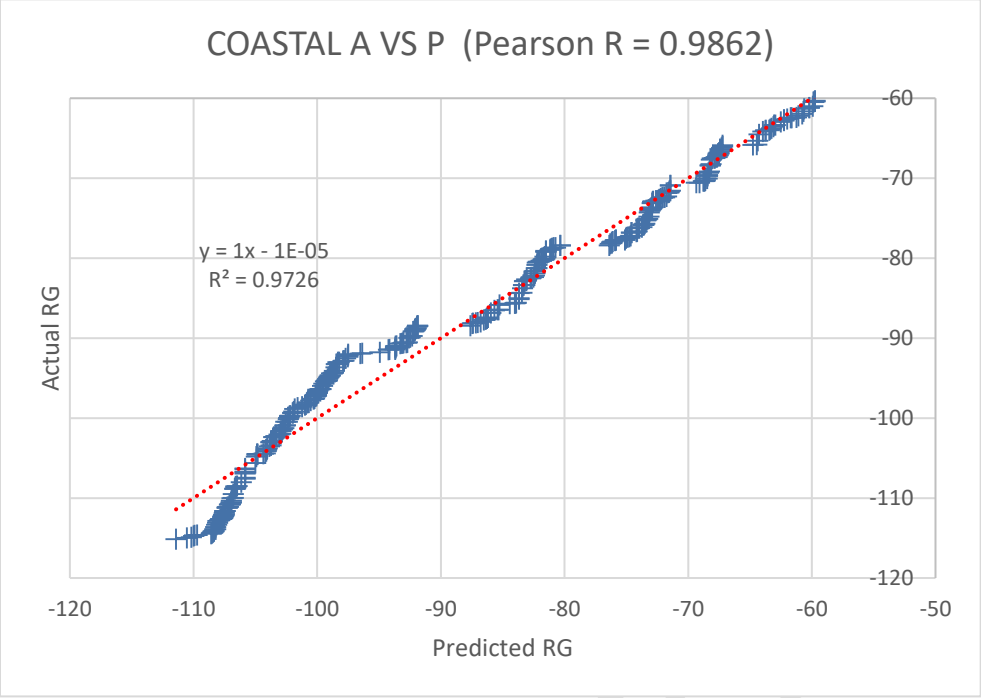

Fig 10. The linear relationship between Actual RG and Predicted RG in the Coastal Region

DERIVED REGION

The correlation coefficient in this region is 0.9902, the correlation is positive. It shows there is a strong linear relationship between Actual RG and Predicted RG. As Actual RG increases, Predicted RG also increases. While R^2 suggests that 98% of changes in Actual RG to changes in Predicted RG, 2% are unexplained which justifies that this model can be used to forecast future values of Refractivity gradients provided that the latitudinal position of ITD is known for stations in the derived region. This also implies the model is more accurate in the derived region by 1% over the coastal region.

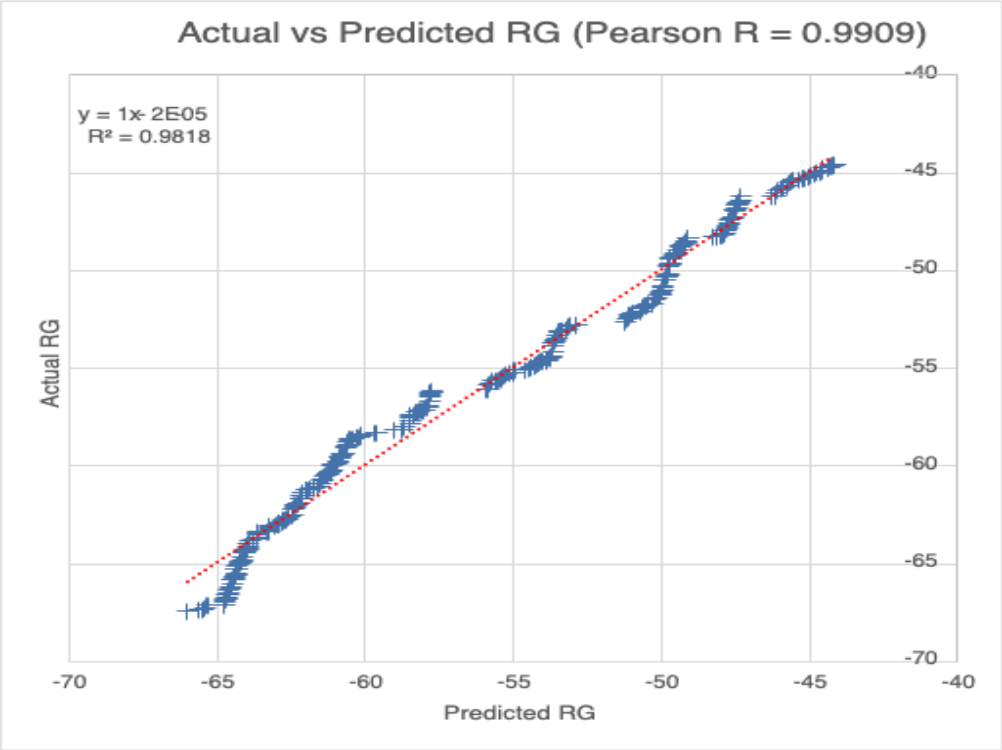

Fig 11. The linear relationship between Actual RG and Predicted RG in DERIVED REGION

Guinea Region

The correlation coefficient in this region is 0.9919, the correlation is positive. It shows there is a stronger linear relationship between Actual RG and Predicted RG. As Actual RG increases, Predicted RG also increases. While R^2 suggests that 98% of changes in Actual RG to changes in Predicted RG, 2% are unexplained which justifies that this model can be used to forecast future values of Refractivity gradients provided that the latitudinal position of ITD is known for stations in the Guinea Savanna region. This also implies the model is more accurate in the Guinea region over the coastal and derived regions.

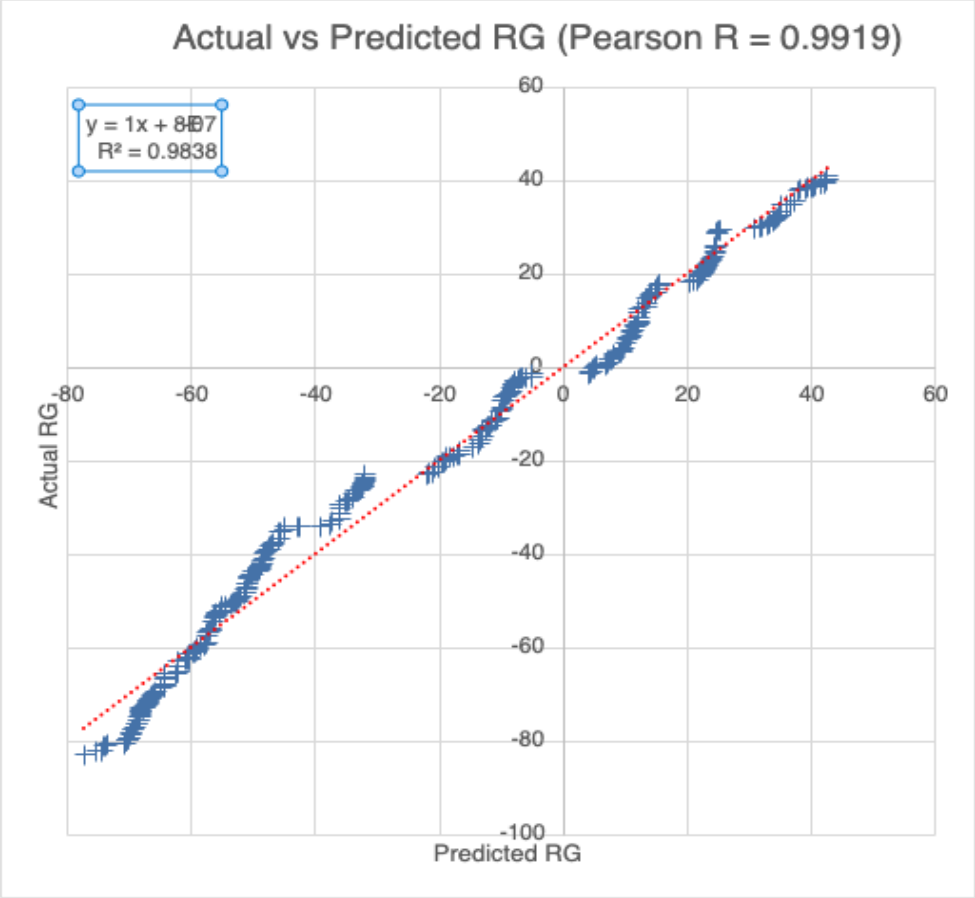

Fig 12. Linear relationship between Actual RG and Predicted RG in **Guinea Region**

Sub-Sahelian Region

The correlation coefficient in this region is 0.9919, the correlation is positive. It shows there is a stronger linear relationship between Actual RG and Predicted RG. As Actual RG increases, Predicted RG also increases. While R^2 suggests that 98% of changes in Actual RG to changes in Predicted RG, 2% are unexplained which justifies that this model can be used to forecast future values of Refractivity gradients provided that the latitudinal position of ITD is known for stations in the Guinea Savanna region. This also implies the model is more accurate in the Sahel region over the coastal and derived regions.

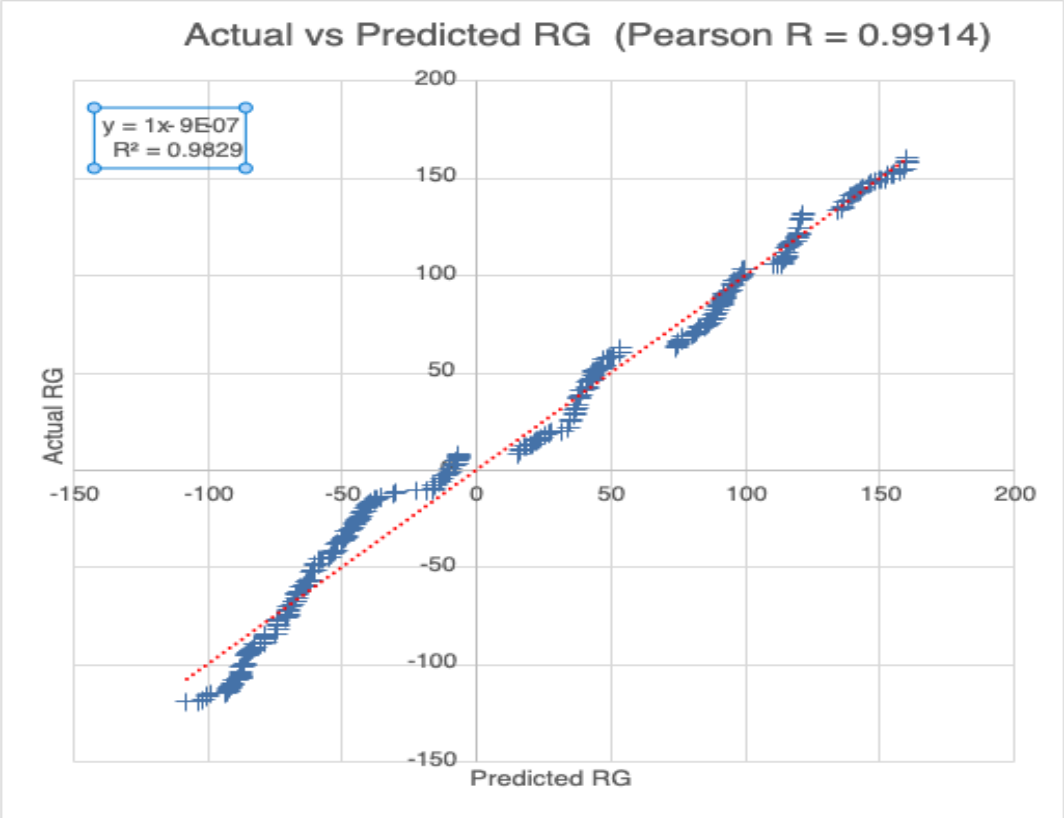

Fig 13. Linear Relationship between Actual RG and Predicted RG in the Sub-Sahelian Region

5. Conclusion

The relationship between refractivity gradients and intertropical discontinuities has been convincingly demonstrated in this work, with differences in refractivity gradients found to be very low during wet seasons and large during dry seasons across all stations, owing to their proximity to the ocean, the stations around the coast have lower refractivity values than other stations. The migration of the intertropical discontinuity (ITD) across all stations has been revealed to influence the distribution of rainfall across all stations. The value of the refractivity gradient reduces throughout the stations as the latitudinal position of ITD increases.

The regression model built in this study showed a positive link between the values of the refractivity gradient and the latitudinal position of the Intertropical discontinuity across Nigeria's four geographical areas. The regression models performed stronger in the Derived and Guinea regions with about 98% accuracy. This would help Radio engineers to plan against anomalous propagations in communication fields and would help

in generating estimates of Refractivity gradients for locations with similar climatic condition of regions studied in this work.

6. References

Adeyemi B. Surface water vapour density and tropospheric radio refractivity linkage over three stations in Nigeria. Journal of Atmospheric and Solar-Terrestrial Physics. 2006 Jun 1;68(10):1105-15.

Emmanuel I, Adeyemi B, Ogolo EO, Adediji AT. Characteristics of the anomalous refractive conditions in Nigeria. Journal of Atmospheric and Solar-Terrestrial Physics. 2017 Nov 1;164:215-21.

Zhang T, Tan G, Bai W, Sun Y, Wang Y, Luo X, Song H, Sun S. A Disturbance Frequency Index in Earthquake Forecast Using Radio Occultation Data. Remote Sensing. 2023 Jun 13;15(12):3089.

Adediji, A. T., Dada J. B. & Ajewole, M. O. (2019). Diurnal, Seasonal and Annual Variation of Microwave Radio Refractivity Gradient over Akure, South West Nigeria. Physical Science International Journal, 23(4): 111. doi:10.9734/PSIJ/2019/v23i430161

Emmanuel I, Adeyemi B, Adedayo KD. Regional variation of columnar refractivity with meteorological variables from climate monitoring satellite application facility (CM SAF) data over Nigeria. International journal of physical sciences. 2013 May 9;8(17):825-34.

Adediji, A.T. and Ajewole, M., 2008. Vertical Profile of Radio Refractivity Gradient in Akure South-West Nigeria. Progress In Electromagnetics Research C, 4, pp.157-168.

Refractivity gradient of the first 1km of the troposphere for some selected stations in six geo-political zones in Nigeria2019IOP Conference Series: Materials Science and Engineering doi: 10.1088/1757-899x/640/1/012087.

Falodun SE, Ajewole MO. Radio refractive index in the lowest 100-m layer of the troposphere in Akure, South Western Nigeria. Journal of Atmospheric and Solar-Terrestrial Physics. 2006 Jan 16;68(2):236-43.

Emmanuel I, Ojo OS, Abe OE, Adedayo KD. Geostatistical distribution of vertical refractivity gradient over Nigeria. Radio Science. 2020 Sep;55(9):1-8.

Dairo OF, Kolawole LB. Radio refractivity gradients in the lowest 100m of the atmosphere over Lagos, Nigeria in the rainy-harmattan transition phase. Journal of Atmospheric and Solar-Terrestrial Physics. 2018 Jan 1;167:169-76.

G. A. Agbo, G. F. Ibeh, D. U. Onah, A. E. Umahi, E. Nnaji and F. C. Ugwuonah, "Application of Neural Network in Atmospheric Refractivity Profile at Markurdi," International Conference on Information, Business and Education (ICIBIT, 2013) Atlantis Press.

S. T. Ogunjo, J. S. Ojo, A. T. Adediji, K. D. Adedayo, and J. B. Dada. Chaos in radio refractivity over Akure, South-Western Nigeria. Book of Proceedings of the 5th Annual Conference of the Nigeria union of Radio Science (NURS), 2013 pp. 56 – 63.

A.T Adediji and S. T. Ogunjo, "Variations in nonlinearity in vertical distribution of microwave radio refractivity" Progress in Electromagnetics Research M,, 36, 2014, PP.177-183.

Willoughby AA, Aro TO, Owolabi IE. Seasonal variations of radio refractivity gradients in Nigeria. Journal of Atmospheric and Solar-Terrestrial Physics. 2002 Mar 1;64(4):417-25.

Dumka UC, Kaskaoutis DG, Francis D, Chaboureau JP, Rashki A, Tiwari S, Singh S, Liakakou E, Mihalopoulos N. The role of the Intertropical discontinuity region and the heat low in dust emission and transport over the Thar Desert, India: A Premonsoon case study. Journal of Geophysical Research: Atmospheres. 2019 Dec 16;124(23):13197-219.

Winker, D.M., Tackett, J.L., Getzewich, B.J., Liu, Z., Vaughan, M.A., Rogers, R.R., (2013), The global 3-D distribution of tropospheric aerosols as characterized by CALIOP,Atmos.Chem. Phys. 13, 3345–3361

Adeyemi B, Ogolo EO. Diurnal and Seasonal variations of surface water vapour density over some meteorological stations in Nigeria. Ife Journal of Science. 2014;16(2):181-9.

Pospichal, B., Karam, D., Crewell, S., Flamant, C., Hünerbein, A., Bock, O., & Saïd, F. (2010). Diurnal cycle of the intertropical discontinuity over West Africa analysed by remote sensing and mesoscale modelling. Quarterly Journal of the Royal Meteorological Society, 136(S1), 92-106. https://doi.org/10.1002/qj.435

Xu, C., Ma, Y., Yang, K., You, C., (2018), Tibetan Plateau impacts on global dust transport in the upper troposphere, J. Climate, doi: 10.1175/JCLI-D-17-0313.1

Yuan, T., Chen, S., Huang, J., Wu, D., Zhang, G., Ma, X., Chen, Z., Luo, Y., Ma, X., (2019), Influence of dynamic and thermal forcing on the meridional transport of Taklimakan desert dust in spring and summer, J. Climate 32, 749-767

Pospichal B, Karam D, Crewell S, Flamant C, Hünerbein A, Bock O, Saïd F. Diurnal cycle of the intertropical discontinuity over West Africa analysed by remote sensing and mesoscale modelling. Quarterly Journal of the Royal Meteorological Society. 2010 Jan;136(S1):92-106.

Redelsperger JL, Thorncroft CD, Diedhiou A, Lebel T, Parker DJ, Polcher J. African Monsoon Multidisciplinary Analysis: An international research project and field campaign. Bulletin of the American Meteorological Society. 2006 Dec;87(12):1739-46.

Schneider T, Bischoff T, Haug GH. Migrations and dynamics of the intertropical convergence zone. Nature. 2014 Sep 4;513(7516):45-53.

Arowolo AV, Oluleye A. Assessing the influence of intertropical discontinuity on total column ozone variation over West Africa. Environmental Science and Pollution Research. 2022 Sep;29(44):66689-704.

Ilesanmi OO. An empirical formulation of an ITD rainfall model for the tropics: a case study of Nigeria. Journal of Applied Meteorology (1962-1982). 1971 Oct 1:882-91.

Zubair M, Haider Z, Khan SA, Nasir J. Atmospheric influences on satellite communications. Przeglad Elektrotechniczny. 2011 Jan 1;87(5):261-4.

Balin I. Measurement and analysis of aerosols, cirrus-contrails, water vapor and temperature in the upper troposphere with the Jungfraujoch LIDAR system. EPFL; 2004.

Emetere ME, Afolalu SA, Abodunrin TJ. Seasonal surface refractivity patterns in the part of Lagos-Nigeria. InIOP Conference Series: Earth and Environmental Science 2021 Feb 1 (Vol. 655, No. 1, p. 012013). IOP Publishing.

Dairo OF, Kolawole LB. Statistical analysis of radio refractivity gradient of the rainy-harmattan transition phase of the lowest 100 m over Lagos, Nigeria. J. Atmos. Sol.-Terr. Phys. 2017.